

A sample of 6C radio sources with virtually complete redshifts. II – optical spectroscopy

Steve Rawlings^{1*}, Steve Eales² and Mark Lacy^{1,3,4}

¹*Astrophysics, Department of Physics, Keble Road, Oxford OX1 3RH, UK*

²*Department of Physics and Astronomy, University of Wales College of Cardiff, P.O. Box 913, Cardiff CF2 3YB, UK*

³*Institute of Geophysics and Planetary Physics, L-413 Lawrence Livermore National Laboratory, Livermore CA 94550, USA*

⁴*Department of Physics, University of California, 1 Shields Avenue, Davis CA 95616, USA*

24 October 2018

ABSTRACT

This is the second of two papers presenting basic observational data on the 6CE sample of extragalactic radio sources. It presents the results of optical spectroscopy which has yielded virtually complete redshift information for the 6CE sample: 56 of the 59 sample members have spectroscopic redshifts which, with the exception of seven cases, are secure. The redshift distribution $N(z)$ is fairly flat over the redshift range $0 \leq z < 2$, with a median redshift of ≈ 1.1 and a high-redshift tail reaching to $z = 3.4$. The highest-redshift ($z > 1.75$) members of the 6CE sample have similar optical spectra and a tight (less than one dex) spread in narrow-Ly α emission line luminosity.

Key words: radio continuum:galaxies – galaxies:active – quasars:general

1 INTRODUCTION

Obtaining spectroscopic redshifts for complete samples of radio sources is a key requirement for a large number of investigations of the radio source population and its cosmic evolution. Such investigations are severely compromised if they are based on a sample selected at a single limiting flux density, for example the 3CRR sample (Laing, Riley & Longair 1983), because of the limited coverage they provide of the 151 MHz luminosity L_{151} versus redshift z plane (e.g. Fig. 1). Studies based only on the 3CRR sample cannot distinguish between correlations with redshift z and correlations with L_{151} , and they cannot straightforwardly measure the relative numbers of radio sources at a given redshift as a function of L_{151} , or conversely the relative numbers at a given L_{151} as a function of z .

To ameliorate this problem we have been seeking complete redshift information for low frequency (151 MHz) selected samples drawn from the 6C and 7C radio surveys (e.g. Rawlings et al. 1998). These

samples greatly increase the coverage of the L_{151} - z plane as illustrated in Fig. 1. In this paper we report on optical spectroscopy of a 6C-based sample first defined by Eales (1985a) and now, as described in this paper, slightly revised. This is the second of two papers aimed at presenting basic observational data on this revised ‘6CE’ sample. The first paper (Eales et al. 1997) presented near-IR images of many members of the sample.

A numbers of papers have made use of the 6CE dataset. Investigations of the inter-correlations between radio properties (e.g. luminosity, projected linear size, spectral index) and redshift can be found in Neeser et al. (1995), Best et al. (1999) and Blundell, Rawlings & Willott (1999). Investigations of the near-IR properties of the combined 6CE/3CRR dataset can be found in Eales et al. (1997) and Roche, Eales & Rawlings (1998). An investigation of the fraction of quasars in low frequency selected complete samples can be found in Willott et al. (2000b). Measurements of the radio luminosity function using the combined 3CRR/6CE/7CRS dataset are presented in Willott et al. (2000c).

*Email: s.rawlings1@physics.ox.ac.uk

Throughout this paper we adopt the follow-

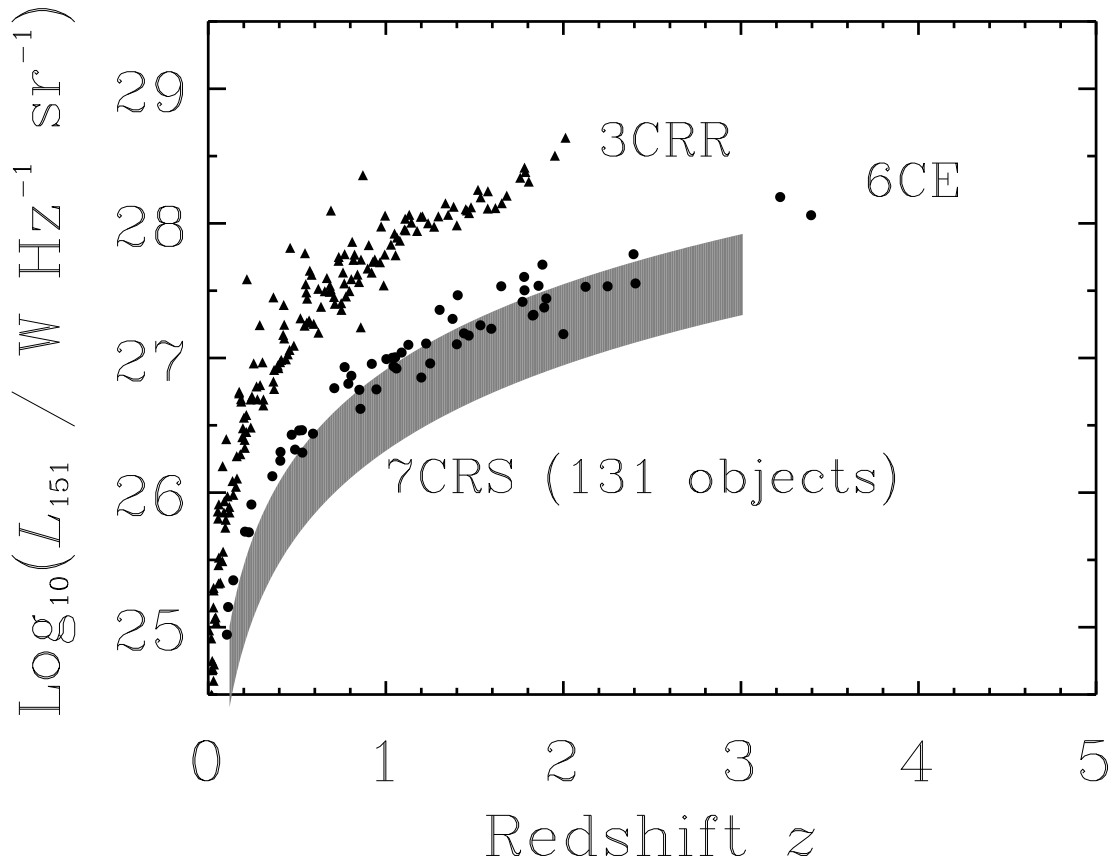


Figure 1. The coverage of the 151 MHz luminosity L_{151} versus redshift z plane for the 3CRR sample (triangles) and the 6CE sample (circles); the shaded region shows the rough location of the 131 members of the 7C Redshift Survey (7CRS; Lacy et al. 1999; Blundell et al. in prep.; Willott et al. in prep).

ing values for the cosmological parameters: $H_0 = 50 \text{ km s}^{-1} \text{ Mpc}^{-1}$, $\Omega_M = 1$ and $\Omega_\Lambda = 0$. B1950.0 coordinates are used and the convention for radio spectral index α is that $S_\nu \propto \nu^{-\alpha}$, where S_ν is the flux density at frequency ν .

2 THE 6CE SAMPLE

2.1 Sample membership

Since the definition of the original 6C sample by Eales (1985a), the flux density scale of the 6C survey has been revised, and a number of programmes of follow-up at radio wavelengths (Naundorf et al. 1992; Law-Green et al. 1995a), and in the near-IR and optical (e.g. Eales et al. 1997; this paper), have allowed us to make a proper assessment of source confusion. As a result, the 151 MHz flux density S_{151} limits of the sample have been slightly altered, and the sample membership has been refined. The final selection criteria of the 6CE sample are as follows:

- $08^{\text{h}}20^{\text{m}}30^{\text{s}} < \text{RA (B1950)} < 13^{\text{h}}01^{\text{m}}30^{\text{s}}$;
- $34^\circ < \text{Dec (B1950)} < 40^\circ$;
- $2.00 \text{ Jy} \leq S_{151} < 3.93 \text{ Jy}$.

The sky area of the sample is 0.102 sr. The region of sky was chosen initially by Eales (1985a) because of overlap with a sample of (408-MHz selected) B2 radio sources studied by Allington-Smith (1982) and it consisted of 67 sources. Eight of these sources are excluded from the (revised) 6CE sample: 6C0825+36, 6C0848+34, 6C0918+36, 6C0955+39 and 6C1106+38 because revised estimates of S_{151} place the 6C catalogue entry below the flux-density limit (Hales, Baldwin & Warner 1988; Hales, Baldwin & Warner 1993); and 6C0951+37, 6C1028+35 and 6C1045+35C because the (integrated) S_{151} 6C catalogue entry results from the confusion of two or more radio sources which, if considered individually, would fall below the flux-density limit (see Law-Green et al. 1995a). There are no new sources in the 6CE sample which therefore comprises 59 radio sources. A summary of key information on

the 6CE sample is provided in Table 1; versions of this table in both ASCII and HTML formats are available from the worldwide-web at <http://www-astro.physics.ox.ac.uk/~sr/6ce.html>.

One of the 59 6CE sources (6C1036+3616) is projected so close to a bright star that any effective optical/near-IR follow-up has so far proved impossible. Of the remaining 58 sources, five are ‘flat-spectrum’ in the sense that their low-frequency radio spectra have indices lower than 0.4 but it is not yet proven that any of these have been promoted into the sample on the basis of Doppler-boosted components.

(1)	(2)	(3)	(4)	(5)	(6)	(7)	(8)	(9)	(10)
	name	S_{151}	α_{151}	Cl	K	z	Line	$\log_{10} L_{\text{line}}$	z ref
	6C0820+3642	2.39	0.82	HEG	18.41 (Eea 5)	1.860	Ly α	36.55	REL
A	6C0822+3417	3.06	0.55	LEG	15.26 (LLA 12)	0.406	[OII]	(35.1)	ALL
	6C0822+3434	2.93	1.19	LEG?	17.71 (Eea 5)	0.768	[OII]	34.78	DSpc
A	6C0823+3758	3.35	0.76	LEG	13.74 (LLA 12)	0.207	[OII]	(< 34.2)	ALL
A	6C0824+3535	2.42	0.41	Q	-	2.249			ASDL
A	6C0825+3452	2.10	0.58	HEG	19.19 (Eea 5)	1.467	[OII]	35.73	EHRpc
A	6C0847+3758	3.07	0.91	HEG	15.05 (LLA 12)	0.407	[OII]	(34.8)	ALL
A	6C0854+3956	2.92	0.65	HEG	15.39 (LLA 12)	0.528	[OII]	(35.3)	ALL
A	6C0857+3907	2.71	0.73	HEG	15.03 (LLA 12)	0.229		(35.1)	ALL
	6C0901+3551	2.07	0.74	HEG	18.29 (Eea 5)	1.904	Ly α	36.67	REW†
A	6C0902+3419	2.14	0.80	HEG	19.70 (Eb 4)	3.395	Ly α	37.00	L
	6C0905+3955	2.82	1.13	HEG	18.48 (Eea 5)	1.882	Ly α	36.31	REL
A	6C0908+3736	2.33	0.53	LEG	12.70 (LLA 12)	0.105	[OII]	(< 34.2)	Wea
A	6C0913+3907	2.27	0.24	Q	-	1.250			La/ASDL
	6C0919+3806	2.72	0.91	LEG	18.20 (Eea 5)	1.650?	CII]?	34.96	REL‡
A	6C0922+3640	3.27	0.58	LEG	12.60 (LLA 12)	0.112	[OII]	(< 34.5)	S
	6C0930+3855	2.21	0.86	LEG?	19.30 (ER 4)	2.395	Ly α	36.10	REL
	6C0943+3958	2.31	0.82	LEG?	18.09 (Eea 5)	1.037	[OII]	35.65	REL
A	6C0955+3844	3.45	0.84	Q	-	1.405			La/ASDL
A	6C1011+3632	2.10	0.74	HEG	18.05 (Eea 5)	1.043	[OII]	35.00	REL
A	6C1016+3637	2.28	0.49	HEG	> 20.30 (Eea 5)	1.892	Ly α	36.01	REL
A	6C1017+3712	2.68	0.62	HEG	18.88 (Eea 5)	1.053	[OII]	35.48	REL
A	6C1018+3729	2.52	1.00	HEG	16.49 (LLA 12)	0.806	[OII]	35.48	ASDL
A	6C1019+3924	2.99	0.65	LEG?	16.64 (LLA 12)	0.921	[OII]	(35.5)	ALL
A	6C1025+3900	2.97	0.54	LEG?	14.48 (LLA 12)	0.361	[OII]	35.46	ASDL
	6C1031+3405	2.33	0.47	HEG	19.30 (ER 4)	1.832	Ly α	36.20	REL‡
A	6C1036+3616	2.81	-	-	-	-	-	-	-
A	6C1042+3912	2.68	0.52	HEG	19.70 (Eea 5)	1.770	Ly α	36.26	REL
A	6C1043+3714	2.62	0.83	LEG?	17.38 (LLA 12)	0.789	[OII]	(36.2)	ALL
	6C1045+3403	2.00	0.59	HEG	18.91 (Eea 5)	1.827	Ly α	36.77	REL

Table 1. A summary of key information on the 6CE sample; the reason for the lack of data on 6C1036+3616 is explained in Sec. 2.1. **Column 1:** ‘A’ indicates that the radio source is also in the B2-selected ‘1-Jy’ sample of Allington-Smith (1982). **Column 2:** name of the 6CE radio source. **Column 3:** 151-MHz flux density from the final versions of the 6C survey (Hales et al. 1998; Hales et al. 1993), and **column 4:** radio spectral index evaluated at rest-frame 151 MHz using a polynomial fit to the multi-frequency data. **Column 5:** classification, Q=quasar and BLRG=broad-line radio galaxy, following the prescription of Willott et al. (1998); and HEG=high-excitation galaxy, LEG=low-excitation galaxy, following the prescription of Jackson & Rawlings (1997) when [OII] is accessible, and using the detection of any line from an at least doubly-ionized ion as a diagnostic in higher-redshift cases; ‘?’ means that the classification is uncertain – object-by-object discussions are presented in Secs. 2.2.1 and 2.2.2. **Column 6:** K -band magnitude of the radio source ID – a reference to the source of this magnitude and the diameter (in arcsec) of the photometric aperture, is given in the brackets; ‘?’ indicates that this K -band detection is significant at only the 2.6σ level; ‘-’ signifies that no K -band photometry is available; references are Ea=Eales et al. (1993a), Eb=Eales et al. (1993b), Eea = Eales et al. (1997), ER = Eales & Rawlings (1996), LLA=Lilly, Longair & Allington-Smith (1985), L89=Lilly (1989). **Column 7:** redshift, ‘?’ means that this value is not yet an unequivocal redshift; ‘-’ indicates that spectroscopy has yet to reveal a redshift; ‘*’ indicates that the galaxy with this redshift is not yet certain to be the correct radio source ID. **Column 8:** Prominent emission line in the existing spectra, a ‘?’ meaning that the line identification is uncertain. **Column 9:** \log_{10} of the line luminosity in units of W, a ‘-’ means the data are inadequate to obtain a line luminosity; brackets denote that the luminosity is estimated from an observed equivalent width (EW) and an r - or R -band magnitude (from either LLA or Eales 1985c); to estimate [OII] limits from the spectra of the low-redshift LEGs studied by Sargent (1973) or Warner et al. (1983), we took $EW < 25 \text{ \AA}$ and $EW < 10 \text{ \AA}$ respectively, a detected [OII] line in a Sargent spectrum is assigned an $EW = 25 \text{ \AA}$. **Column 10:** reference to spectroscopy/spectrophotometry: Apc, J. Allington-Smith *priv. comm.*; ALL, Allington-Smith et al. (1985); ASDL, Allington-Smith et al. (1988); DSpc, M. Dickinson & H. Spinrad *priv. comm.*; EH, Eracleous & Halpern (1994); EHRpc, S. Eales, C. Haniff & S. Rawlings *priv. comm.*; ERWpc, S. Eales, S. Rawlings & S. Warren *priv. comm.*; La, Lahulla et al. (1991); L, Lilly (1988); LMRSpc, M. Lacy, S. Maddox, S. Rawlings & S. Serjeant *priv. comm.*; REL, this paper; REW, Rawlings, Eales & Warren (1990); S, Sargent (1973); VT, Vermeulen & Taylor (1995); Wea, Warner et al. (1983); WW, Wills & Wills (1979). A † indicates that the line flux has been measured from a new spectrum presented in this paper. A ‡ means that the previously reported redshift is incorrect (see object-by-object notes in Secs. 2.2.1 and 2.2.2).

(1)	(2)	(3)	(4)	(5)	(6)	(7)	(8)	(9)	(10)
	name	S_{151}	α_{151}	Cl	K	z	Line	$\log_{10} L_{\text{line}}$	z ref.
	6C1045+3553	2.07	0.76	LEG?	16.33 (Eea 5)	0.851?	[OII]?	(35.4)	LMRSpç
	6C1045+3513	3.03	0.20	Q	16.77 (Eea 5)	1.594	-		ERWpc‡
A	6C1100+3505	2.26	0.58	HEG	18.33 (Eea 5)	1.440	[NeIV]	35.73	Apc
A	6C1108+3956	2.10	0.74	LEG	16.27 (LLA 12)	0.590	[OII]	(34.9)	ASDL
A	6C1113+3458	2.33	0.52	HEG?	18.29 (L 8)	2.406?	Ly α ?	35.97	REL
	6C1123+3401	3.40	-0.27	LEG?	17.92 (Eea 5)	1.247?	CII]?	34.59	REL
A	6C1125+3745	2.07	0.79	Q	17.46 (LLA 12)	1.233	[OII]	< 35.15	REL
A	6C1129+3710	2.36	0.51	HEG?	17.52 (Eea 5)	1.060	[OII]		REL
A	6C1130+3456	3.20	0.57	LEG	15.76 (LLA 12)	0.512	[OII]	(35.1)	ALL
	6C1134+3656	2.07	0.73	HEG	19.40 (ER 5)	2.125	Ly α	36.62	REW†
A	6C1141+3525	2.40	0.82	HEG	18.72 (Eea 5)	1.781	Ly α	37.00	ASDL
A	6C1143+3703	2.06	0.24	LEG?	19.83? (Eea 5)	-	-	-	REL
A	6C1148+3638	3.21	0.69	LEG?	14.63 (LLA 12)	0.141	[OII]	(> 33.8)	S
A	6C1148+3842	3.83	0.64	Q	-	1.303	-	-	WW
	6C1158+3433	2.12	0.50	LEG	-	0.530?	[OII]?	34.60	REL
A	6C1159+3651	2.20	0.50	LEG?	17.42 (L89 8)	-	-	-	REL
A	6C1204+3708	3.92	0.61	HEG	19.29 (Eea 5)	1.779	Ly α	37.00	REL
A	6C1204+3519	3.43	0.54	HEG	17.97 (Eea 5)	1.376	CIV	35.73	REL
	6C1205+3912	3.83	0.76	LEG?	-	0.243	[OII]	(34.9)	S
A	6C1212+3805	2.14	0.49	LEG?	17.74 (Eea 5)	0.947?	[OII]?	35.20	REL
	6C1213+3504	2.39	0.02	Q	-	0.857	[OII]	(35.4)	VT
A	6C1217+3645	2.40	0.74	HEG?	17.27 (Eea 5)	1.089?	[OII]?	34.81	REL
A	6C1220+3723	2.52	0.59	Q	15.30 (LLA 12)	0.489	[OIII]	(36.2)	ALL
A	6C1230+3459	2.90	0.42	HEG	18.40 (Eea 5)	1.533	[NeIV]	35.59	ASDL
	6C1232+3942	3.27	0.93	HEG	17.80 (Ea 11)	3.221	Ly α	36.73	REW
A	6C1255+3700	3.66	0.49	Q	15.59 (LLA 12)	0.710	[OIII]	(36.1)	EH‡
A	6C1256+3648	2.88	0.60	HEG?	17.75 (Eea 5)	1.127	[OII]	35.37	REL
	6C1257+3633	2.40	0.84	HEG	17.51 (Eea 5)	1.003	[OII]	36.58	REL
A	6C1301+3812	3.46	0.63	HEG	14.66 (LLA 12)	0.470*	[OII]	(35.5)	ALL

Table 1. (cont).

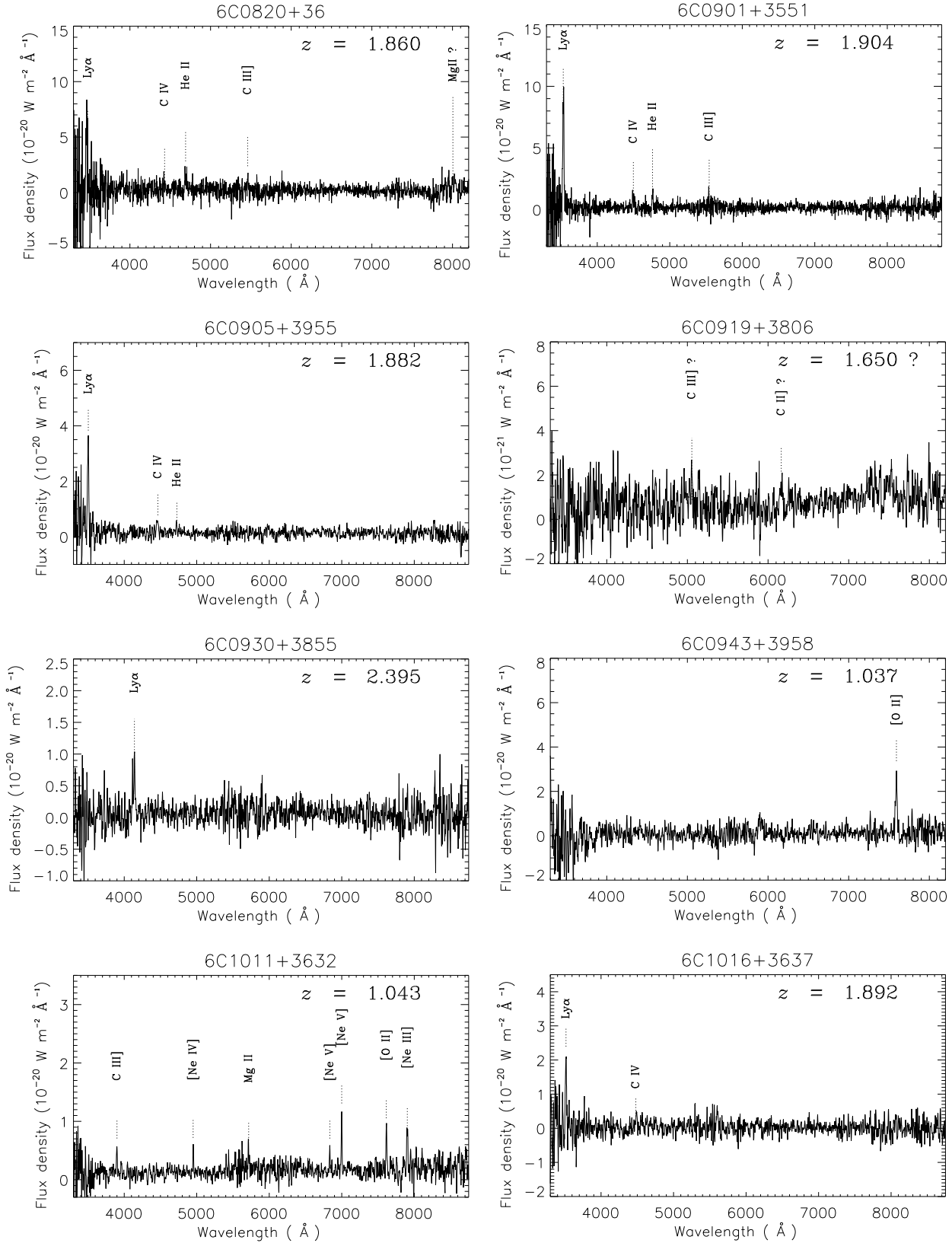


Figure 2. Spectra of the 6CE WHT targets with definite or possible spectral features. The synthetic aperture used to extract 1D spectra from the 2D data was typically defined by the full-width at zero-intensity of a cross-cut through the data, excepting the cases of 6C1158+3433 and 6C1217+3645 for which a full-width at half-maximum aperture was used.

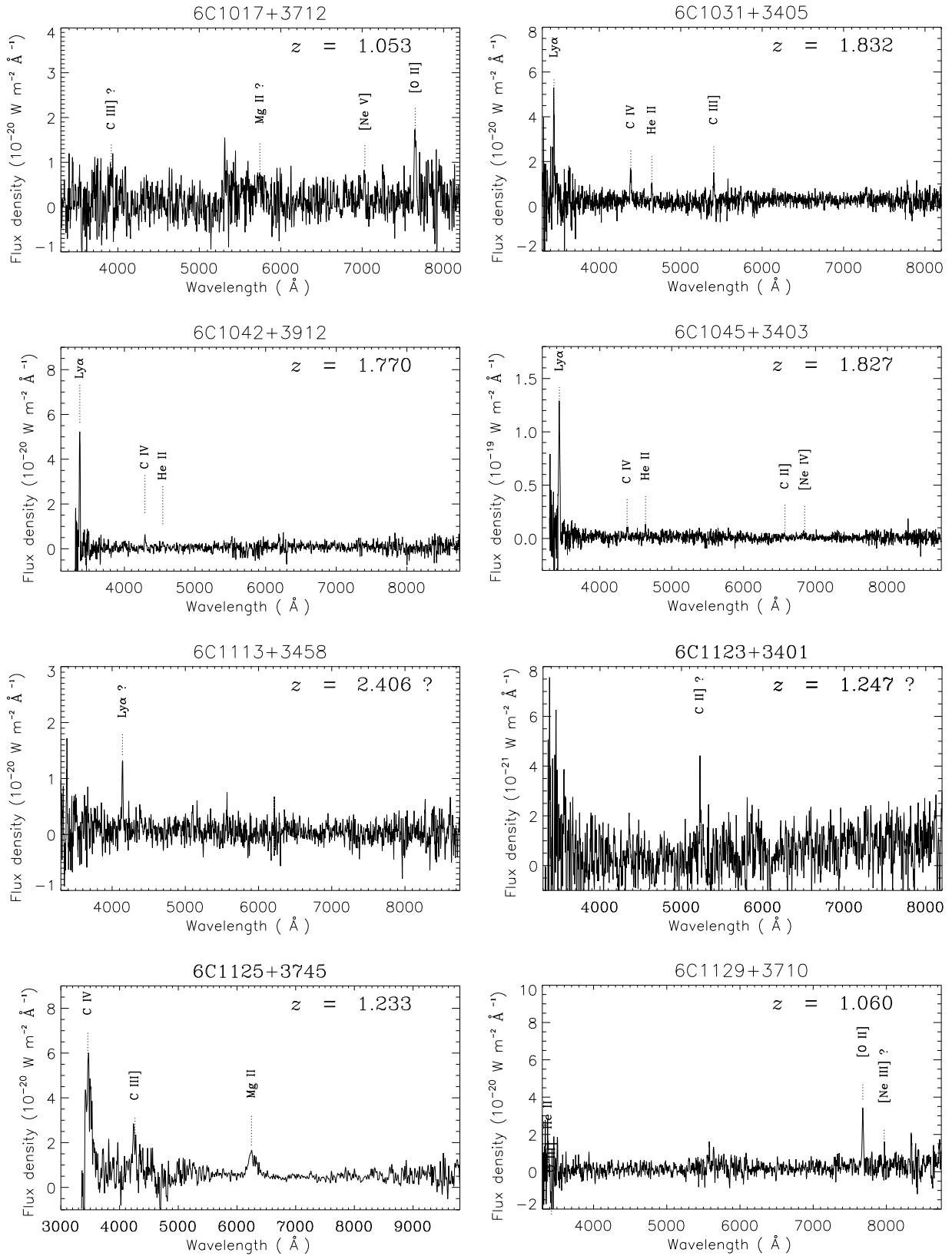


Figure 2. (cont)

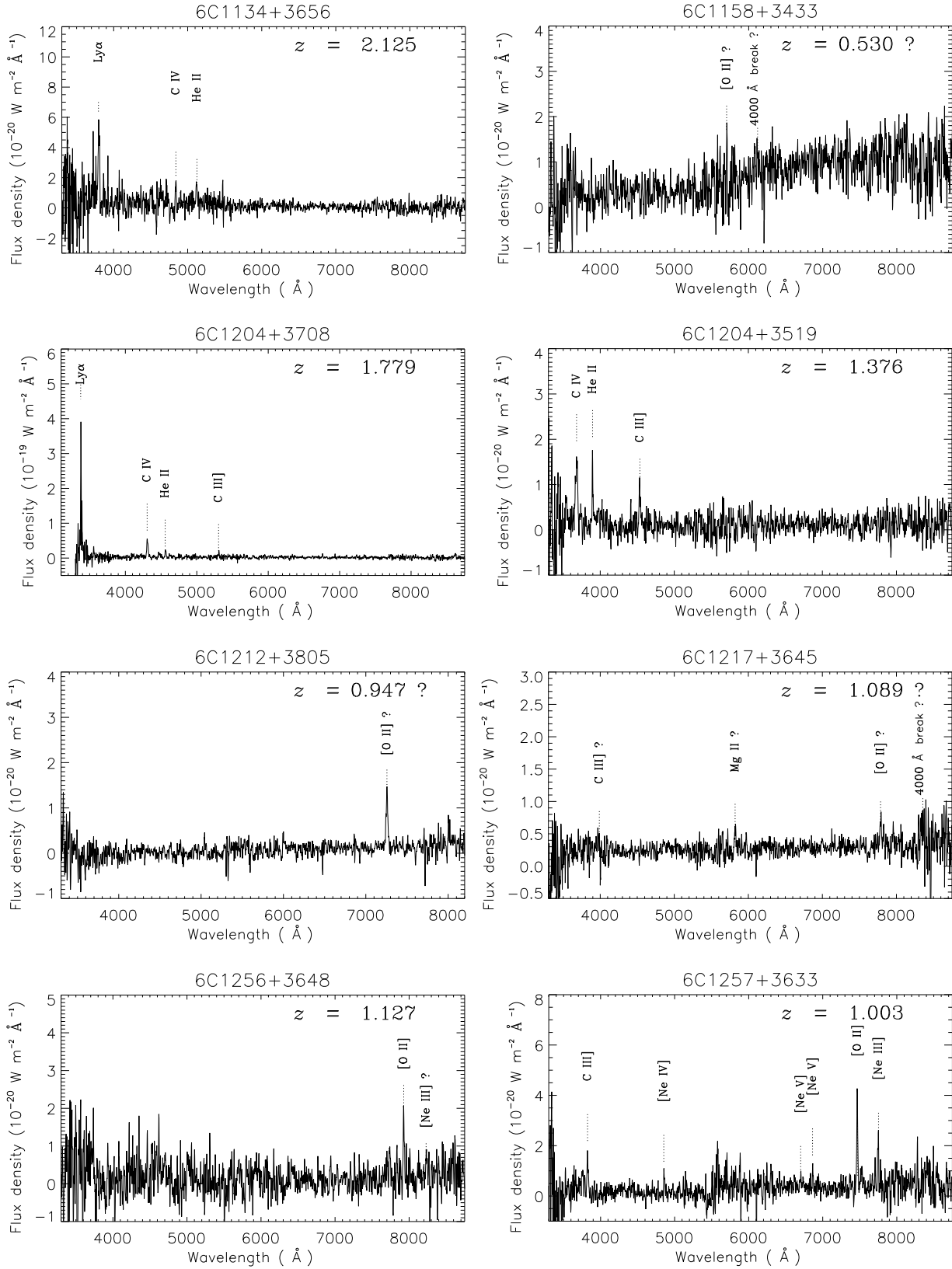


Figure 2. (cont)

2.2 Observations and spectroscopic redshifts

The optical spectra presented in this paper were mostly obtained during the course of two WHT observing runs in Jan. 1994 and Jan. 1995 using the ISIS spectrometer; some data taken with the FOS-II spectrograph in Jan. 1992 are also presented (see Cotter, Rawlings & Saunders 1996 for details of the observational-setup used in this run). A journal of all these observations is presented in Table 2. All ISIS observations used the R158R and R158B gratings with the beam split using the 5400-Å dichroic; the blue-arm detector was the TEK1 chip on both runs, the red-arm detector was the EEV3 chip in 1994 and the TEK2 chip in 1995. These setups produced continuous spectral coverage from the blue atmospheric cut-off to ≈ 8750 Å in 1994, and to ≈ 8200 Å in 1995. The pixel scales for the TEK and EEV chips were 0.358 and 0.336 arcsec pixel⁻¹ respectively.

Observations and data analysis followed the standard methods described by Lacy & Rawlings (1994). We offset from nearby bright stars to either optical or radio positions, choosing the position angle (PA) of the slit either on the basis of encompassing companion optical objects or to coincide with the radio axis. All the targets were observed below an air mass of 1.2, and all but two were observed below an air mass of 1.1. All the data presented here were taken in photometric conditions with the seeing close to 1 arcsec. In nearly all cases spectral features, emission lines and/or spectral breaks, were detected and the reduced 1D spectra are presented in Fig. 2. For cosmetic purposes, most of the spectra have been smoothed by replacing the value of each spectral bin by the average of the values in the bin and its two neighbours. All measurements from the spectra were made prior to this process, and the results of these measurements are tabulated in Table 3.

2.2.1 Notes on the 6CE WHT targets

6C0820+36 We obtain an unequivocal redshift from the spatially-extended emission lines seen in Fig. 2: the alignment of the slit with the radio axis meant that we missed the companion object to the south-west of the radio galaxy in the image of Eales et al. (1997).

6C0901+3551 Our WHT spectrum confirms the tentative redshift obtained by Rawlings, Eales & Warren (1990).

6C0905+3955 Our WHT spectroscopy of this giant radio galaxy has been reported previously by Law-Green et al. (1995b): the Ly α flux tabulated in Table 3 is significantly higher than the value given in Table 2 of Law-Green et al. because it is evaluated from the total-light spectrum. The Ly α emission extends from the continuum-emitting galaxy towards the shorter western radio lobe with a secondary peak approximately midway between the radio galaxy and

a companion object visible in the near-IR image of Law-Green et al.

6C0919+3806 Our WHT spectrum does not yield an unequivocal redshift for this object although two plausible emission features in the spectrum are consistent with $z = 1.650$: the redshift given in Table 1 of Eales & Rawlings (1996) is almost certainly incorrect. Continuum is detected from 3800 Å, and it remains roughly flat in F_λ until ≈ 6100 Å, and then rises (roughly $\propto \lambda^3$) into the red: the lack of a detected Lyman-limit cut-off means the redshift is less than about 3.2. We note broad similarities between this spectrum and those of the old, red radio galaxies studied by Dunlop (1999), and by identifying the continuum inflexion with a rest-frame wavelength ≈ 2600 Å, we obtain a redshift estimate $z \sim 1.3$.

6C0930+3855 Our WHT spectrum contains a single doubled-peaked line which, since it matches well with lines detected in the near-IR by Eales & Rawlings (1996), is securely identified with Ly α . The cause of the double-peaked structure is most probably HI-absorption in the host galaxy.

6C0943+3958 Our WHT spectrum contains a single bright emission line, but recent deeper spectroscopy in the optical (P. Best & S. Rawlings, *priv. comm.*) has confirmed the redshift obtained if this feature is associated with [OII]3727. The location of the strong line (and weak continuum) emission along the slit confirms that the radio galaxy lies much closer to the eastern than the western radio hotspot in agreement with the near-IR position given by Eales et al. (1997).

6C1011+3632 The spectrum of this galaxy is rich in high-ionization emission lines which are neither spatially nor spectrally resolved.

6C1016+3637 We aligned the slit through two plausible optical IDs marked on the radio map presented by Law-Green et al. (1995a). Our WHT spectroscopy detects continuum emission from both these objects but separate line emission from about half-way between them; both candidate IDs are therefore likely to be spurious, with the true ID having a Dec (1950.0) of +36 37 46. Since this ID is likely to lie along the radio axis it is possible that we have missed some fraction ($\lesssim 50$ per cent) of the line emission. In Table 1 we have placed a limit on the K -band magnitude of the true ID equal to the magnitude of the northern optical object, since this was detected at $\approx 3\sigma$ in the near-IR image of Eales et al. (1997).

6C1017+3712 We targeted the optical position given by Lilly (1989) confirming the redshift he referenced to H. Spinrad (*priv. comm.*).

6C1031+3405 Our 1995 spectrum yields an unambiguous redshift for object ‘b’ of Eales & Rawlings (1996) [the redshift given in their Table 1 is incorrect] and its strong emission lines, together with its location near the radio midpoint, mean that this is almost certainly the correct radio galaxy ID. Object ‘a’, an R -band ID proposed by Eales (1985b), was

observed in 1994 and has a tentative redshift of 0.449 from a weak but definite line at 7255 Å, assumed to be [OIII]5007, and a possible line at ≈ 5413 Å, assumed to be [OII]3727.

6C1042+3912 The Ly α emission line from this object is detected in the far blue, but two confirming emission lines are also evident in the 2D blue-arm spectrum.

6C1045+3403 The redshift of this object is based on five emission lines.

6C1113+3458 There is just one emission feature in the spectrum of this object which because of its wavelength and huge equivalent width we take to be Ly α . The lack of any confirming features renders this redshift insecure.

6C1123+3401 There is only one definite emission line in the spectrum of this object so its redshift is not yet secure. In F_λ the spectrum rises roughly $\propto \lambda^4$ from $\lambda \approx 5000$ Å until $\lambda \approx 7200$ Å then flattens off. Together with the near-IR photometry (Eales et al. 1997), this produces a spectral energy distribution that is reminiscent of the old red galaxies studied by Dunlop (1999); by identifying the continuum flattening with a rest-frame wavelength ≈ 3250 Å, we estimate a redshift ~ 1.2 , which means that a plausible identification of the emission line is CII]2326. At this redshift [OII]3727 would lie just beyond the wavelength span of the 1995 WHT spectroscopy and the relatively poor quality of the 1992 WHT (FOS-II) data means that the lack of any detected feature is not a strong argument against the veracity of the tentative redshift.

6C1129+3710 Our WHT spectrum contains a single bright emission line, but additional deeper optical spectroscopy (P. Best & S. Rawlings, *priv. comm.*) detects additional lines which confirm the redshift obtained if this feature is associated with [OII]3727.

6C1134+3656 Our WHT spectrum confirms the tentative redshift obtained by Rawlings et al. (1990), although their claimed CIII]1909 feature is not seen in the new spectrum.

6C1143+3703 We observed this source in both 1994 and 1995 (with the same pointing position, but different slit PAs) but detected neither continuum nor lines: excepting the regions of the strongest night-sky emission lines, we can put a 5σ limit on any emission line at the $\sim 1 \times 10^{-19}$ Wm $^{-2}$ level. Being only marginally detected at K -band, this object is the faintest object in the 6CE sample.

6C1158+3433 The spectrum of this object is relatively poor because it was a short exposure taken near twilight. There is a tentative detection of a single emission line which, if taken as [OII]3727, is consistent with a plausible 4000-Å spectral break. The precise redshift of this object is therefore uncertain but both the spectral shape and magnitude are those expected for a giant elliptical galaxy at $z \sim 0.5$.

6C1159+3651 In 1994 we observed at a PA selected to include a companion object about 6 arcsec

to the east (Lilly 1989) and in 1995 at the PA of the radio source. In all the red-arm spectra we see continuum from the ID amounting to $R \sim 24$, in reasonable agreement with the photometry of Lilly, but there are no emission lines in the coadded data to a 5σ limit of $\sim 1 \times 10^{-19}$ Wm $^{-2}$ (excepting the regions of the strong night-sky emission lines). The continuum is roughly flat in F_λ , although at the signal-to-noise ratio of the detected continuum it is impossible to search for any spectral breaks. Note the following: (i) the redshift given for this source in Table 1 of Eales & Rawlings (1996) is almost certainly incorrect; and (ii) the near-IR photometry (Lilly 1989) may include some contribution from the companion object (from which we detected featureless continuum in 1994).

6C1204+3708 Since this is a large (51.5 arcsec) radio source, we began our blind exposure with a 5-arcsec wide slit, and on seeing no emission lines in the first red exposure, we widened the slit to 7 arcsec for the second red exposure, and more importantly (given the much higher ratio of read noise to sky noise in the blue) for the remainder of the blue exposure. We detected strong emission lines in the blue-arm spectrum from a location along the slit consistent with the position of the near-IR ID of Eales et al. (1997). The line parameters for Ly α are rather uncertain because a cosmic ray event effects two pixels near to its location. We also detected the object near the western hotspot in the Eales et al. image: if the single emission line detected from this object is [OII]3727, its redshift is $z = 0.864$ making it foreground to the radio galaxy.

6C1204+3519 This object provides a salutary lesson on the dangers of assuming that a bright, highly-extended emission line in the blue is always Ly α : the detection of three clear emission lines leaves no doubt that the brightest line, which is extended over 6 arcsec, is CIV not Ly α . The HeII and CIII] lines peak at the location of the continuum, and are also detected in a continuum-free blob ≈ 2 arcsec (approximately) to the north; the line fluxes of these two components are roughly equal, although there is additional diffuse material, at least in CIV. In the red-arm spectrum there is also evidence for MgII emission from the blob (although none is clearly detected in the total-light spectrum of Fig. 2). There are hints in both the HeII and CIII] emission that the blob is blue-shifted by ≈ 750 km s $^{-1}$ with respect to the continuum-emitting object, which might also help explain the broad width of the CIV feature in the total-light spectrum. These observations might explain two unusual features of this object: (i) relatively unusually for the 6CE sample, the near-IR emission is well aligned with the radio axis (Eales et al. 1997), perhaps caused by two near-IR objects coinciding with the spatial peaks in the optical line emission; and (ii) the relatively large offset between the putative radio central component (Law-Green et al. 1995a) and the position of the optical ID — either the ‘radio core’ is actually a knot in the jet, coincident with the emission-line blob, or

the active nucleus lies within the blob approximately 2-arcsec to the north of an optically-brighter galaxy.

6C1212+3805 The spectrum of this object shows only a single strong emission line which we associate with [OII]3727 since the spectrum has red continuum detected on both sides of the line, and the spectral energy distribution rises rapidly into the near-IR (Eales et al. 1997; see also Maxfield et al. 1995) where the ID is as bright as a typical 6CE galaxy at $z \sim 1$. We eliminated the possibility that the single bright line is Ly α by detecting the ID in a deep (3×600 s) *B*-band image with the WHT Prime Focus Camera on 19 Apr. 1996 since this pass-band would lie below the Lyman limit if the line were Ly α . The line emission is spatially resolved but not in an obviously asymmetric way with respect to the continuum. Our slit also encompassed the companion galaxy to the north-west in the image of Eales et al. from which we detect spatially-extended red continuum but no emission lines.

6C1217+3645 Three highly tentative emission features are detected which line up well with a redshift supported by a far-from-convincing 4000-Å break. The emission from this object is spatially unresolved in seeing of about 1 arcsec, but although the signal-to-noise ratio is too low to be certain, there are no hints that the putative CIII] and MgII features are broad as would be the case if, as suggested by Benítez et al. (1995), this object should be re-classified as a quasar. Note, further, that the 1.24-arcsec seeing, near-IR image of this galaxy is resolved (Roche et al. 1998). The radio properties of this source are highly unusual (Best et al. 1999), and one might speculate that the compact nature of the ID, and its relatively blue colour are further indications that this source is anomalous within the sample, one possibility being that it is a radio halo source in a rich cluster rather than a classical double.

6C1256+3648 Our WHT spectrum contains only a single definite emission line, but additional deeper optical spectroscopy (P. Best & S. Rawlings, *priv. comm.*) detects additional lines which confirm the redshift obtained if this feature is associated with [OII]3727. The emission line region extends from the galaxy over the entire southern radio lobe; no line emission is seen towards the northern lobe. The slit also encompassed a galaxy ≈ 17 arcsec to the north-east of the radio galaxy, visible as a similar magnitude galaxy in the image of Eales et al. (1997): we detect an [OII] line in this galaxy at a similar redshift, so this galaxy is a companion to the radio galaxy in line with the suggestion of Lilly (1989) that this field is reminiscent of the core of a rich cluster.

6C1257+3633 The extension of the [OII]3727 emission is towards the south eastern radio lobe which shows very little radio polarization (Best et al. 1999). The extended emission shows a distinct blob ~ 3 arcsec in this direction which, following the near-IR/radio registration of Best et al., puts it slightly

beyond a prominent knot in the radio emission. Although there is no clear MgII emission in the total-light spectrum (Fig. 2), there are hints of MgII emission in the 2D spectrum at the position of the blob, but no hints of high-ionization lines suggesting a lower effective ionization parameter for this emission.

2.2.2 Notes on other 6CE sources

6C0825+3452 Inspection of the NVSS image (Condon et al. 1998) of this radio source shows that there is a confusion problem which means that the 151-MHz flux density S_{151} of the main source is likely to lie uncomfortably close to the 6CE sample flux density limit. In the absence of evidence to the contrary we assume that the main source still lies above the S_{151} lower limit. There are two faint near-IR objects close to the position of this radio source: Eales et al. (1997) favoured the brighter south-eastern object as the ID, but the subsequent detection of an inverted radio central component at the position of the fainter north-western object (Best et al. 1999) means that this is more likely to be the correct near-IR counterpart. The redshift was obtained by blind spectroscopy.

6C1045+3553 The redshift is based on a single emission line presumed to be [OII].

6C1045+3513 The nature and redshift of the ID of this source reported by Naundorf et al. (1992) is incorrect: spectroscopy shows that as originally suspected by Eales (1985b) the object is a quasar and lies at $z = 1.594$, not at $z \sim 0.7$. The cause of the confusion is the optical/near-IR colour of the object which is similar to that of an elliptical galaxy at $z \sim 0.7$: the compact near-IR image of Eales et al. (1997) shows that the red colour is the result of light reddening of a quasar nucleus just like 3C318, the nature and redshift of which has recently similarly been revised (Willott, Rawlings & Jarvis 2000a).

6C1255+3700 The redshift reported for this source by Warner et al. (1983) is incorrect – we have estimated an observed equivalent width of ≈ 50 Å for the [OIII]5007 line from the spectrum of Eracleous & Halpern (1994) which also shows clear broad H β .

6C1301+3812 No radio central component has been detected for this object, so, as discussed by Allington-Smith, Lilly & Longair (1985), identification of the radio source with their galaxy ‘B’ remains an unproven assumption.

2.3 Objects without secure spectroscopic redshifts

Inspection of Table 1 shows that, excluding the object obscured by a bright star, only two 6CE objects (6C1143+3703 and 6C1159+3651) lack any sort of spectroscopic redshifts. This remarkable (97 per cent) level of redshift completeness is unprecedented at these flux density levels (e.g. McCarthy et al. 1996),

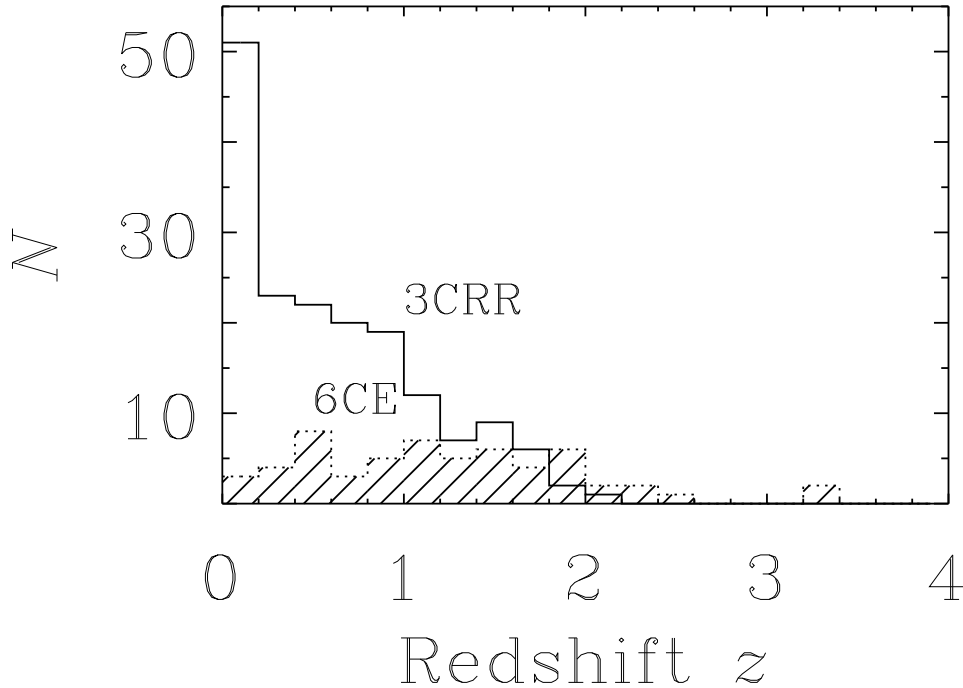


Figure 3. Histograms of the redshift distributions $N(z)$ of the 6CE sample (dotted line and cross-hatched) and the 3CRR sample (full line and open). The bin width on each histogram is $\Delta z = 0.2$.

and provides compensation for the relatively modest sample size. One of these troublesome objects (6C1159+3651) is relatively bright in the near-IR, but faint in the optical, properties that are characteristic of a galaxy in the redshift range $0.8 \leq z \leq 2$ and we take $z = 1.4$ here. The other object (6C1143+3703) is faint at K so, rather arbitrarily given the scatter in the $K - z$ relation at faint magnitudes (e.g. Eales et al. 1997), we take $z = 2$.

The 56 spectroscopic redshifts given in Table 1 are not yet all secure. In four cases (6C1045+3553, 6C1113+3458, 6C1123+3401, 6C1212+3805) this is because the redshift depends on the correct identification of a single emission line; in a further three cases (6C0919+3806, 6C1158+3433, 6C1217+3645) this is because there are no clear-cut spectral features in the observed spectrum, but typically several tentative features consistent with a single redshift. Longer spectroscopic exposures of all these seven objects would be useful. In one further case (6C1301+3812) there is some doubt about whether the measured redshift is for the host galaxy of the 6C radio source.

2.4 The redshift distribution

The redshift distribution of the 6CE sample is compared with that of the 3CRR sample in Fig. 3. Note the very different redshift distributions resulting from the nature and redshift dependence of the radio luminosity function and the observable comoving volume on our light cone (see Willott et al. 2000c). The median redshift of the 6CE sample is ≈ 1.1 with a maximum redshift ≈ 3.4 , while the 3CRR sample has a median redshift ≈ 0.55 and a maximum redshift ≈ 2 .

Object	Date	Position (1950.0)		Exposures	Slit Width and PA (arcsec) (°)	
6C0820+3642	27/01/95	08 20 33.89	+36 42 28.3 (r)	(1 × 900B, 1 × 900R)	3	155 (r)
6C0901+3551	08/01/94	09 01 25.10	+35 51 00.8 (r)	(1 × 1800B, 2 × 900R)	3	120 (r)
6C0905+3955	06/01/94	09 05 04.95	+39 55 34.9 (c)	(1 × 1800B, 2 × 900R)	3	103 (i)
	08/01/94	09 05 04.95	+39 55 34.9 (c)	(1 × 1800B, 2 × 900R)	3	103 (i)
6C0919+3806	28/01/95	09 19 08.00	+38 06 51.7 (c?)	(2 × 1800B, 4 × 900R)	2	151 (r)
6C0930+3855	07/01/94	09 30 00.76	+38 55 07.4 (r)	(1 × 1800B, 2 × 900R)	3	0 (r)
6C0943+3958	27/01/95	09 43 13.67	+39 58 11.2 (r)	(1 × 600B, 1 × 600R)	3	100 (r)
6C1011+3632	07/01/94	10 11 16.91	+36 32 12.4 (c)	(1 × 1500B, 1 × 900 + 1 × 600R)	2	0 (r)
6C1016+3637	07/01/94	10 16 58.45	+36 37 49.7 (o)	(1 × 1800B, 2 × 900R)	3	167 (o)
6C1017+3712	27/01/95	10 17 44.70	+37 12 08.0 (o)	(1 × 600B, 1 × 600R)	3	45 (r)
6C1031+3405	06/01/94	10 31 44.21	+34 04 54.7 (o)	(1 × 1800B, 2 × 900R)	3	135 (r)
	27/01/95	10 31 44.29	+34 04 57.9 (r)	(1 × 1800B, 1 × 1800R)	3	135 (r)
6C1042+3912	07/01/94	10 42 23.73	+39 12 25.2 (r)	(1 × 1800B, 2 × 900R)	3	110 (r)
6C1045+3403	06/01/94	10 45 24.18	+34 03 37.9 (r)	(1 × 1800B, 2 × 900R)	3	110 (r)
6C1113+3458	06/01/94	11 13 47.65	+34 58 46.5 (r)	(1 × 1800B, 2 × 900R)	3	18 (r)
	08/01/94	11 13 47.65	+34 58 46.5 (r)	(1 × 1200B, 1 × 1200R)	3	18 (r)
6C1123+3401	29/01/92	11 23 43.09	+34 01 57.0 (r)	(2 × 900B, 2 × 900R)	4	93 (v)
	28/01/95	11 23 43.09	+34 01 57.0 (r)	(1 × 1800B, 2 × 900R)	2	176 (v)
	31/01/95	11 23 43.09	+34 01 57.0 (r)	(1 × 1800B, 2 × 900R)	2	115 (v)
6C1125+3745	29/01/92	11 25 49.77	+37 45 25.3 (o)	(2 × 900B, 2 × 900R)	4	87 (r)
6C1129+3710	06/01/94	11 29 55.45	+37 10 51.9 (r)	(1 × 1000B, 1 × 900R)	3	138 (v)
6C1134+3656	08/01/94	11 34 28.60	+36 56 30.0 (r)	(1 × 1800B, 2 × 900R)	3	130 (r)
6C1143+3703	07/01/94	11 43 01.23	+37 03 07.4 (r)	(1 × 1800B, 1 × 1800R)	2	68 (v)
	28/01/95	11 43 01.23	+37 03 07.4 (r)	(1 × 1550B, 1 × 1550R)	2	90 (v)
6C1158+3433	08/01/94	11 58 19.50	+34 33 28.9 (o)	(1 × 600B, 1 × 600R)	3	90 (v)
6C1159+3651	09/01/94	11 59 20.94	+36 51 36.2 (r)	(1 × 1800B, 2 × 900R)	3	100 (o)
	27/01/95	11 59 20.94	+36 51 36.2 (r)	(1 × 1800B, 1 × 1800R)	2	32 (r)
6C1204+3708	09/01/94	12 04 22.08	+37 08 17.7 (r)	(1 × 1200B, 2 × 600R)	5-7	107 (r)
6C1204+3519	07/01/94	12 04 59.32	+35 19 46.8 (o)	(1 × 1800B, 2 × 900R)	2	12 (r)
6C1212+3805	27/01/95	12 12 26.04	+38 05 31.0 (r)	(1 × 1800B, 1 × 1800R)	2.7	130 (r)
6C1217+3635	09/01/94	12 17 40.16	+36 45 45.4 (o)	(1 × 1200B, 2 × 600R)	2	95 (o)
	27/01/95	12 17 40.16	+36 45 45.4 (r)	(1 × 1800B, 1 × 1800R)	1.8	40 (r)
6C1256+3648	06/01/94	12 56 44.75	+36 48 08.4 (o)	(1 × 1800B, 2 × 900R)	3	50 (r)
6C1257+3633	09/01/94	12 57 08.78	+36 33 11.5 (c)	(1 × 1200B, 2 × 600R)	3	138 (r)

Table 2. Journal of optical spectroscopy of the 6CE targets. The letter in brackets after the target position denotes its origin: ‘c’ denotes a radio central component; ‘r’, the centre of an extended radio structure; ‘o’, the position of the optical ID; ‘i’, the position of an infrared ID. Exposures gives the time in s of each exposure in the blue (B) and red (R) arms. The letter in brackets after the PA denotes whether the slit alignment was chosen to match the radio (‘r’) axis, or the major axis of infrared (‘i’) or optical (‘o’) structures, or whether the choice was made irrespective of the object properties (‘v’), normally at an angle close to the parallactic angle at the time of observation.

Object	Line	λ_{rest} (Å)	λ_{meas} (Å)	Continuum (10^{-22} W m $^{-2}$ Å $^{-1}$)	Flux (% Error) (10^{-19} W m $^{-2}$)	Extent (arcsec)	Comments
6C0820+3642	Ly α	1216	3464	≤ 10.0	15.0 (30)	7	FWHM unreliable near CR removed
	CIV	1549	4420	20.0	1.2 (50)		
	HeII	1640	4691	25.0	3.3 (50)		
	CIII]	1909	5463	25.0	1.6 (50)		
6C0901+3551	Ly α	1216	3533	≤ 10.0	18.8 (15)	1	FWHM = 0-1300
	CIV	1549	4498	10.0	2.6 (50)		
	HeII	1640	4764	10.0	2.6 (30)		
	CIII]	1909	5538	25.0	1.0 (50)		
6C0905+3955	Ly α	1216	3505	≤ 10.0	8.4 (30)	5	FWHM = 0-1300
	CIV	1549	4457	15.0	2.0 (40)		
	HeII	1640	4719	20.0	0.5 (50)		
6C0919+3806	CIII]?!]	1909	5050	5.0	0.2 (50)		
	CII]?!]	2326	6174	5.0	0.5 (50)		
6C0930+3855	Ly α	1216	4116/4140	≤ 5.0	3.0 (30)	< 1	Double-peaked
6C0943+3958	[OII]	3727	7593	10.0	6.9 (15)	4	FWHM = 400-900
6C1011+3632	CIII]	1909	3899	20.0	1.3 (30)	< 1	FWHM=0-400
	[NeIV]	2424	4955	20.0	1.0 (20)		
	MgII	2798	5711	25.0	0.6 (50)		
	[NeV]	3346	6835	20.0	0.5 (30)		
	[NeV]	3426	6998	20.0	1.7 (15)		
	[OII]	3727	7617	20.0	1.5 (20)		
	[NeIII]	3869	7904	20.0	2.0 (20)		
6C1016+3637	Ly α	1216	3516	≤ 10.0	4.2 (20)	4	FWHM =0-1200
	CIV	1549	4488	≤ 10.0	1.0 (30)		
6C1017+3712	[NeV]	3426	7025	10.0	1.4 (50)	5	FWHM=750-1100
	[OII]	3727	7651	10.0	4.5 (30)		
6C1031+3405	Ly α	1216	3440	10.0	7.0 (30)	< 1	FWHM=0-800
	CIV	1549	4386	30.0	2.4 (30)		
	HeII	1640	4646	25.0	1.0 (30)		
	CIII]	1909	5404	20.0	1.7 (40)		
6C1042+3912	Ly α	1216	3368	≤ 10.0	8.5 (30)	< 1	FWHM=0-1100
	CIV	1549	4291	≤ 10.0	1.0 (30)		
	HeII	1640	4544	≤ 10.0	0.6 (50)		
6C1045+3403	Ly α	1216	3435	≤ 10.0	25.8 (15)	5	FWHM=800-1800
	CIV	1549	4382	15.0	1.5 (30)		
	HeII	1640	4635	15.0	1.2 (50)		
	CII]	2326	6567	10.0	0.6 (60)		
	[NeIV]	2424	6835	20.0	0.6 (50)		

Table 3. Measurements obtained from the WHT spectra of 6CE radio sources. The ‘?’ denotes an uncertain line identification and the ‘!’ denotes a feature which is plausibly spurious. Errors on the line fluxes represent $\approx 90\%$ confidence intervals expressed as a percentage of the best line flux estimate; for the strongest lines these are dominated by roughly equal contributions from uncertainties in fixing the local continuum level, and from the absolute flux calibration (and plausible slit losses). The spatial extents of the emission lines were estimated by evaluating the full-width zero-intensity of a cross-cut through the emission line, deconvolved from the seeing. Line widths (given in units of km s $^{-1}$) were estimated from the FWHM of the best Gaussian fit to each line, the lower value of a range assumes the line-emitting region fills the slit, and the higher value assumes that it is broadened only by the seeing. ‘CR contam’ is short-hand for cosmic-ray contamination.

Object	Line	λ_{rest} (Å)	λ_{meas} (Å)	Continuum (10^{-22} W m $^{-2}$ Å $^{-1}$)	Flux (% Error) (10^{-19} W m $^{-2}$)	Extent (arcsec)	Comments
6C1113+3458	Ly α ?	1216	4142	≤ 10.0	2.2 (20)	3	FWHM = 0-900
6C1123+3401	CII]?	2326	5227	6.0	0.4 (50)		
6C1125+3745	CIV	1549	3471	77.0	48.0 (30)	< 1	FWHM \sim 10000
	CIII]	1909	4237	80.0	9.0 (50)		
	MgII	2798	6249	65.0	15.0 (25)		
6C1129+3710	[OII]	3727	7678	45.0	8.2 (30)	7	FWHM = 0-700
	[NeIII]?!]	3869	7974	45.0	1.2 (60)		
6C1134+3656	Ly α	1216	3800	≤ 20.0	13.0 (30)	15	FWHM=1000-1700
	CIV	1549	4839	25.0	2.0 (40)		
	HeII	1640	5121	30.0	2.6 (40)		
6C1158+3433	[OII]?!]	3727	5704	65.0	2.5 (50)	< 1	FWHM unreliable
6C1204+3708	Ly α	1216	3379	20.0	47.0 (40)	4	CR contam FWHM=1200-1400
	CIV	1549	4305	35.0	11.5 (25)		
	HeII	1640	4635	20.0	3.7 (30)		
	CIII]	1909	5308	25.0	2.1 (40)		
6C1204+3519	CIV	1549	3681	20.0	4.5 (25)	6	FHWM=2000-2500 CR contam?
	HeII	1640	3894	25.0	1.5 (50)		
	CIII]	1909	5404	20.0	1.6 (40)		
6C1212+3805	[OII]?	3727	7256	10.0	3.0 (20)	2	FWHM=550-950
6C1217+3645	CIII]?!]	1909	3965	30.0	0.7 (60)	< 1	CR contam
	MgII?!]	2798	5830	25.0	0.7 (60)		
	[OII]?!]	3727	7793	30.0	0.9 (60)		
6C1256+3648	[OII]	3727	7926	20.0	3.0 (40)	6	FWHM=0-500
	[NeIII]?!]	3869	8232	25.0	1.0 (60)		
6C1257+3633	CIII]	1909	3825	20.0	2.9 (40)	5	FWHM=0-500
	[NeIV]	2424	4855	15.0	1.3 (50)		
	[NeV]	3346	6705	40.0	0.5 (60)		
	[NeV]	3426	6862	35.0	1.2 (50)		
	[OII]	3727	7465	35.0	6.4 (20)		
	[NeIII]	3869	7748	40.0	3.2 (30)		

Table 3. (cont).

2.5 Emission line properties

At redshifts > 1.75 the only 3CRR objects known are, in terms of their radio luminosity, amongst the most extreme objects on our light cone: the 16 $z > 1.75$ 6CE objects are typically ~ 1 dex less radio luminous. Thirteen of these 16 objects lie in very restricted bands of luminosity and redshift, $1.75 \leq z \leq 2.45$ and $27.3 \leq \log_{10}(L_{151}) < 27.8$, and we will take their optical properties to be characteristic of ‘high-redshift 6CE sources’. The two extreme luminosity (and redshift) 6CE sources have been studied in detail elsewhere (6C0902+3419 by, for example, Lilly 1988, Eales et al. 1993b and Carilli 1995; and 6C1232+3942 by Eales et al. 1993a), and the lowest luminosity $z > 1.75$ object is distinct in its radio properties (its projected linear size is more than 1 dex lower than all other 6CE objects $z > 1.75$) and as discussed in Sec. 2.3, is one of the two 6CE sources without a spectroscopic redshift.

As well as spanning narrow ranges of L_{151} and z , the thirteen high-redshift 6CE sources also have strikingly similar optical properties. Excepting 6C0824+3535, the objects are narrow-line radio galaxies rather than quasars, and for the radio galaxies the distribution in $L_{Ly\alpha}$ luminosities $L_{Ly\alpha}$ is very narrow: from Table 1 we find $\log_{10} L_{Ly\alpha} = 36.45 \pm 0.36$. The tight spread in $\log_{10} L_{Ly\alpha}$ is presumably a manifestation of the well-known correlation between narrow-line and radio luminosities (e.g. Willott et al. 1999). Eleven of the twelve relevant 6CE radio galaxy spectra are presented in this paper (Sec. 2.2) and their apparent homogeneity encouraged us to create a composite spectrum which is hopefully representative of a high- z 6CE radio source. This composite was constructed by: (i) changing the wavelength scale of each spectrum to place each object at redshift zero, ensuring each had the same binning in wavelength; (ii) scaling each de-redshifted spectrum to equalize the $Ly\alpha$ fluxes; and (iii) taking a bin-by-bin average with an iterative sigma-clipping rejection algorithm (with the clip set at $\pm 1.5\sigma$). The composite is shown in Fig. 4; the line fluxes relative to $Ly\alpha$ of CIV and HeII are 0.13 and 0.08 respectively, and there are marginally significant detections of the NV and CIII] lines. The CIII] line is clearly detected in at least four of the objects making up the composite, and its low signal-to-noise ratio in Fig. 4 is probably partially due to its location (at high redshift) within the spectral region of the dichroic cross-over for the WHT observations. The rest-frame equivalent widths of $Ly\alpha$, CIV and HeII are within a factor of two of 450, 70 and 30 Å respectively. These results are in good quantitative agreement with the composite spectrum presented by McCarthy (1993) which, since it was calculated from an independent but similar dataset (3C galaxies plus radio galaxies with similar low frequency flux densities to the 6CE sample), shows that there does appear

to be such a thing as a generic UV spectrum of radio-luminous high-redshift galaxies.

2.6 Quasar fraction

The low fraction of quasars in the 6CE sample was first noticed and discussed by Eales (1985b,c). There are only three quasars out of the 18 6CE objects in the $27.3 \leq \log_{10}(L_{151}) < 27.8$ luminosity bin whereas amongst the 41 similarly radio-luminous 3CRR sources, between 14 and 16 (depending on how one classifies 3C22 and 3C41; see Simpson, Rawlings & Lacy 1999) are quasars, i.e. a fraction ≈ 0.4 . Using a combined 3CRR/6CE/7CRS dataset, Willott et al. (2000b) have argued that this fraction is virtually independent of L_{151} and z above a critical value of $\log_{10}(L_{151}) \approx 26.5$. Taking 0.4 as the probability that a given source is viewed as a quasar, the Binomial probability of finding three or fewer 6CE quasars out of 18 6CE objects is about 3 per cent.

One possible reason for this (marginally significant) deficit of quasars is that at the higher redshifts probed by the 6CE sample (see Fig. 1) quasar nuclei may be more easily hidden by dust: perhaps partly because optical spectra probe shorter rest-frame wavelengths, and perhaps partly because of an intrinsically larger fraction of reddened lines-of-sight at high redshift (e.g. Willott et al. 2000a). Just one of the luminous 6CE radio galaxies needs to be a reddened quasar for the binomial probability of the low quasar fraction in 6CE to rise to ~ 10 per cent. Note also that, at the highest radio luminosities and redshifts, one of the two 6CE galaxies is 6C0902+3419 which, as pointed out by Carilli (1995), has radio properties which are consistent with a jet orientation as close to the line-of-sight as a lower-redshift 3CRR quasar. We conclude that the low quasar fraction observed in the 6CE sample, although still plausibly an artefact of small number statistics, hints at one or more redshift-dependent effects that warrant further investigation in a larger sample of high- z radio sources.

ACKNOWLEDGEMENTS

We are extremely grateful to a large number of collaborators who have, over the years, devoted effort and observing time to the quest for complete redshift information for the 6CE sample, namely: Jeremy Allington-Smith, Philip Best, Mark Dickinson, Chris Haniff, Steve Maddox, Richard Saunders, Steve Serjeant, Hy Spinrad and Steve Warren. We thank Katherine Blundell, Duncan Law-Green, Patrick Leahy, Tony Lynas-Gray and Chris Willott for their practical help compiling data on the 6CE sample. We also thank an anonymous referee for comments which helped to improve the organization of this paper. The William Herschel Telescope (WHT) is operated on the island of La Palma by

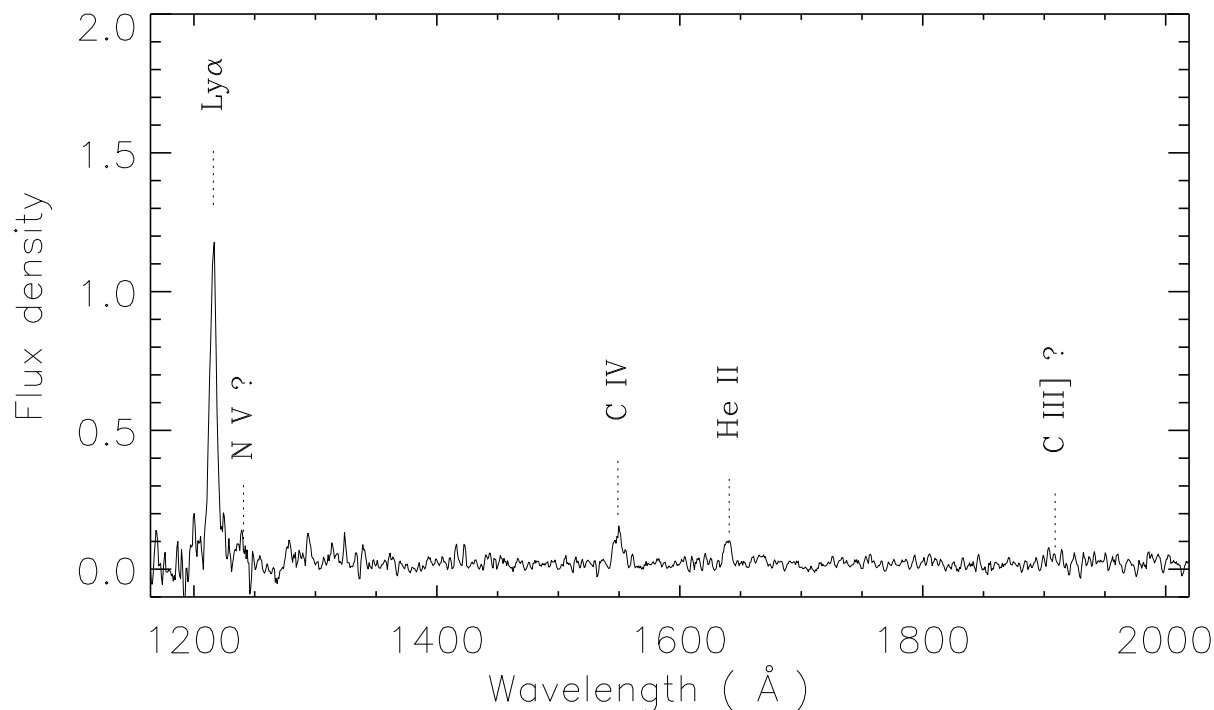


Figure 4. Composite spectrum resulting from the combination of the 11 spectra of $z > 1.75$ 6CE galaxies discussed in Sec. 2.2 with $z > 1.75$; the method of combination is described in Sec. 2.5, and the resultant spectrum has been smoothed with a 3-bin boxcar filter. The flux density is measured in units of $\text{W m}^{-2} \text{Å}^{-1}$ with an arbitrary normalization.

the Isaac Newton Group in the Spanish Observatorio del Roque de los Muchachos of the Instituto de Astrofísica de Canarias. This research has made use of the NASA/IPAC Extragalactic Database, which is operated by the Jet Propulsion Laboratory, Caltech, under contract with the National Aeronautics and Space Administration.

REFERENCES

- Allington-Smith J.R., 1982, MNRAS, 199, 611
 Allington-Smith J.R., Lilly. S.J., Longair, M.S., 1985, MNRAS, 213, 243
 Allington-Smith J.R., Spinrad H., Djorgovski S., Liebert J., 1988, MNRAS 234, 1091
 Benítez N., Martínez-González E., González-Serrano J.I., Cayón L., 1995, MNRAS, 297, 405
 Best P. N., Eales S. A., Longair M. S., Rawlings, S., Röttgering H. J. A., 1999, MNRAS, 303, 616-640
 Blundell K.M., Rawlings S., Willott C.J., 1999, AJ, 117, 677
 Carilli C.L., 1995, A & A, 298, 77
 Condon J. J., Cotton W. D., Greisen E. W., Yin Q. F., Perley R. A., Taylor G. B., Broderick J. J., 1998, AJ, 115, 1693
 Cotter G, Rawlings S., Saunders R., 1996, MNRAS, 281, 1081
 Dunlop J.S., 1999, in The Most Distant Radio Galaxies, eds. H. J. A. Röttgering, P. N. Best, and M. D. Lehnert, p14
 Eales S.A., 1985a, MNRAS, 217, 149
 Eales S.A., 1985b, MNRAS, 217, 167
 Eales S.A., 1985c, MNRAS, 217, 179
 Eales S.A. & Rawlings S., 1996, ApJ, 460, 68
 Eales S.A., Rawlings, S., Dickinson M., Spinrad H., Hill G. J., Lacy, M., 1993a, ApJ, 409, 578
 Eales S.A., Rawlings S., Law-Green D., Cotter G., Lacy M., 1997, MNRAS, 291, 593.
 Eales S., Rawlings S., Puxley P., Rocca-Volmerange B., Kuntz K., 1993b, Nature, 363, 140
 Eracleous M. & Halpern J.P., 1994, ApJS, 90, 1
 Hales S.E.G., Baldwin J.E., Warner, P.J., 1988. MNRAS, 234, 919
 Hales S.E.G., Baldwin J.E., Warner, P.J., 1993. MNRAS, 263, 25
 Jackson N., Rawlings S., 1997, MNRAS, 286, 241
 Lacy M. & Rawlings S., 1994, MNRAS, 270, 833
 Lacy M., Rawlings S., Hill G.J., Bunker A.J., Ridgway S.E., Stern, D., 1999, MNRAS, 308, 1096
 Lahulla J.F., Merighi R., Vettolani G., Vigotti M., 1991, A&AS, 88, 525
 Laing R.A., Riley J.M., Longair M.S., 1983, MNRAS, 204, 151
 Law-Green J.D.B. et al., 1995a, MNRAS, 274, 939
 Law-Green J.D.B., Eales S.A., Leahy J.P., Rawlings S., Lacy M., 1995b, MNRAS, 277, 995

- Lilly S.J., 1988, ApJ, 333, 161
Lilly S.J., 1989, ApJ, 340, 77
Lilly S.J., Longair M.S., Allington-Smith J.R., 1985, MNRAS, 215, 37
Maxfield L., Thompson D., Djorgovski S., Vigotti M., Gru-eff G., 1995, PASP, 107, 369
McCarthy P.J., 1993, ARAA, 31, 639
McCarthy P. J., Kapahi V. K., van Breugel W., Persson, S. E., Athreya, R., Subrahmanya, C. R., 1996, ApJS, 107, 19
Naundorf C.E., Alexander P., Riley J.M., Eales, S.A., 1992, MNRAS, 258, 647
Neeser, M. J., Eales, S. A., Law-Green J. D., Leahy, J. P. & Rawlings, S., 1995, ApJ, 451, 76
Rawlings S., Blundell K.M., Lacy M., Willott C.J., Eales S.A., 1998, in *Observational Cosmology with the New Radio Surveys*, p171
Rawlings S., Eales S.A., Warren S.J., 1990, MNRAS, 243, 14
Roche N., Eales S., Rawlings S., 1998, MNRAS, 297, 405
Sargent W.L.W., 1973. ApJ, 182, L13
Simpson C., Rawlings S., Lacy M., 1999, MNRAS, 306, 828
Vermeulen R.C. & Taylor G.B., 1995, AJ, 109, 1983
Warner P.J., Riley J.M., Eales S.A., Downes A.J.B, Baldwin J.E., 1983, MNRAS, 204, 1279
Willott C.J, Rawlings S., Blundell K.M., Lacy M., 1998, MNRAS, 300, 625
Willott C.J, Rawlings S., Blundell K.M., Lacy M., 1999, MNRAS, 309, 1017
Willott C.J., Rawlings S., Blundell K.M., Lacy M. 2000b, MNRAS, 316, 449
Willott C.J., Rawlings S., Blundell K.M., Lacy M., Eales S.A., 2000c, MNRAS, in press, astro-ph/0010419
Willott C.J., Rawlings S., Jarvis M., 2000a, MNRAS, 313, 217
Wills B.J., Wills D., 1979, ApJS, 41, 689